of precise measurements of quantum yield, and slight differences between the absorption spectrum of bound vs. free ligand. Nevertheless, the approximate distance obtained does strongly suggest that changes in protein conformation upon binding transition-state analogues occur in areas of the protein fairly remote from the actual binding site.

That only negligible quench is obtained with purine riboside is not surprising since the absorption spectrum (maximum at 263 nm) does not overlap the protein emission spectrum to any significant degree.

Conclusion. Consistent with kinetic and equilibrium data, the conformation of adenosine deaminase changes to accomodate binding of analogues of the substrate transition state. This conformation change, as reflected in the change in solvent accessibility of residues likely to be remote from the actual binding site, is the same for transition-state analogues which differ greatly in their affinity. Resonance energy transfer between emitter and ligand successfully explains the differing abilities of the ligands to quench the enzyme's intrinsic fluorescence upon formation of complexes.

ACKNOWLEDGMENTS

We are grateful to Dr. Elliot Elson for suggesting to us that we do these experiments and for his valuable comments on interpretation of the results.

REFERENCES

Anderson, C. M., Steinkamp, R. E., McDonald, R. C., & Steitz, T. A. (1978) *J. Mol. Biol. 123*, 207-209.
Burstein, E. A., Vedenkina, N. S., & Ivkova, M. N. (1973) *Photochem. Photobiol. 18*, 263-279.
Chothia, C., Lesk, A. M., Dodson, G. G., & Hodgkin, D. C. (1983) *Nature (London) 302*, 500-505.
Eftink, M. R., & Ghiron, C. A. (1976) *Biochemistry 15*, 672-680.
Frieden, C., Kurz, L. C., & Gilbert, H. R. (1980) *Biochemistry 19*, 5303-5309.
Huber, R., & Bennett, W. S. (1983) *Biopolymers 22*, 261-279.
Janin, J., & Wodak, S. J. (1983) *Prog. Biophys. Mol. Biol. 42*, 21-78.
Kronman, M. J., & Holmes, L. G. (1971) *Photochem. Photobiol. 14*, 113-134.
Kurz, L. C., & Frieden, C. (1983) *Biochemistry 22*, 382-389.
Lehrer, S. S. (1976) in *Biochemical Fluorescence: Concepts* (Chen, R. F., & Edelhoch, H., Eds.) Vol. 2, pp 515-539, Marcel Dekker, New York.
Lehrer, S. S., & Leavis, P. C. (1978) *Methods Enzymol. 49*, 222-237.
Lesk, A. M., & Chothia, C. (1984) *J. Mol. Biol. 174*, 175-191.
Longworth, J. W. (1971) in *Excited States of Proteins and Nucleic Acids* (Steiner, R. F., & Weinryb, I., Eds.) pp 319-484, Plenum Press, New York.
Parker, C. A. (1968) *Photoluminescence of Solutions*, pp 220-222, Elsevier, New York.
Phelan, J., McEvoy, F., Rooney, S., & Brady, T. G. (1970) *Biochim. Biophys. Acta 200*, 370-377.
Rao, A. G., & Neet, K. E. (1982) *Biochemistry 21*, 6843-6849.
Stryer, L. (1978) *Annu. Rev. Biochem. 47*, 819-846.
Wolfenden, R. (1976) *Annu. Rev. Biophys. Bioeng. 5*, 271-306.
Wolfenden, R. (1978) in *Transition States of Biochemical Processes* (Gandour, R. D., & Schowen, R. L., Eds.) pp 555-575, Plenum Press, New York.
Wolfenden, R., Wentworth, D. F., & Mitchell, G. N. (1977) *Biochemistry 16*, 5071-5077.

Interaction of Pyrophosphate Moieties with α-Helixes in Dinucleotide Binding Proteins

Rik K. Wierenga, Marc C. H. De Maeyer, and Wim G. J. Hol*

Laboratory of Chemical Physics, University of Groningen, Nijenborgh 16, 9747 AG Groningen, The Netherlands
Received July 13, 1984

ABSTRACT: A detailed analysis has been carried out of the binding of dinucleotide pyrophosphate moieties to those proteins where helixes play an important role in the binding. For this analysis, the three-dimensional structures and amino acid sequences of six proteins interacting with three different dinucleotides were available. As glutathione reductase binds two dinucleotides, seven enzyme–dinucleotide complexes have been studied. In all these complexes the pyrophosphate moiety is located near the N-terminus of at least one α-helix: the "dinucleotide binding helix". In dihydrofolate reductase two helixes interact with the pyrophosphate of NADP. Only two common characteristics of all complexes are observed: (i) the occurrence of a glycine at the N-terminus of the helix and (ii) the favorable interaction of the α-helix dipole with the negatively charged pyrophosphate moiety. In virtually every other respect, the dinucleotide binding by dihydrofolate reductase differs from the mode of binding by the five other proteins. The helixes of these five proteins have been grouped together as "category I" dinucleotide binding helixes. The six category I helixes form part of a compact $\beta\alpha\beta$ unit of highly similar structure and very dissimilar sequences. Nevertheless, a characteristic fingerprint for the sequence of this unit can be deduced. Only the ADP moieties of the dinucleotides occupy very similar positions with respect to these compact $\beta\alpha\beta$ units. Therefore, an appropriate name for these units would be "ADP binding $\beta\alpha\beta$ folds".

During the last decade, intriguing observations on the similarity in structure and in dinucleotide binding properties of a number of enzymes that are very different in amino acid sequence have been reported (Rao & Rossmann, 1973; Rossmann et al., 1974, 1975; Ohlsson et al., 1974; Matthews et al., 1979; Wierenga et al., 1983; Birktoft & Banaszak, 1985). These structural investigations have been one of the cornerstones of the generalization by Hol et al. (1978) that

0006-2960/85/0424-1346$01.50/0

Table I: Summary of Relevant Data of the Six Structures Used in the Comparison

enzyme	cofactor	source	code	M_r	source of coordinates[a]	resolution (Å)	ref: structure	ref: sequence
alcohol dehydrogenase	NAD	horse liver	ADH	2 × 41 000	*b*	2.9	Eklund et al., 1981	Jörnvall, 1970
lactate dehydrogenase	NAD	dogfish muscle	LDH	4 × 36 000	PDB (3LDH)	3	White et al., 1976	Taylor, 1977
glyceraldehyde–phosphate dehydrogenase	NAD	lobster muscle	GPD	4 × 36 000	PDB (1GPD)	3	Moras et al., 1975	Davidson et al., 1967
p-hydroxybenzoate hydroxylase	FAD	*Pseudomonas fluorescens*	PHBH	2 × 43 000	*c*	2.5	Wierenga et al., 1979	Weijer et al., 1982
glutathione reductase	FAD and NADP	human erythrocytes	GRS	2 × 53 000	PDB (2GRS)[d]	2.5	Schulz et al., 1982	Krauth-Sieghel et al., 1982
dihydrofolate reductase	NADP	*L. casei*	DHFR	1 × 18 000	PDB (3DFR)[e]	1.7	Bolin et al., 1982	Bitar et al., 1977

[a] PDB, Protein Data Bank (Bernstein et al., 1977). PDG identifiers are given in parentheses. [b] The ADH/NAD coordinate set was given to us by Drs. C.-I. Brändén and H. Eklund. [c] The PHBH coordinates were partly refined. The current *R* factor is 34%. [d] The coordinates of NADP were given to us by Dr. G. E. Schulz. [e] Completely refined coordinate set, *R* = 15%.

the α-helix dipole, interacting favorably with the negatively charged pyrophosphate moiety, contributes significantly to the formation of these dinucleotide–enzyme complexes. Brändén (1980) has also discussed the remarkable similarities in the mode of dinucleotide binding by this group of proteins and has suggested that the occurrence of crevices near "switch points" of β-sheets are important for the common characteristics observed. These correspondences in binding crevices do still allow variation in the position of the dinucleotides, more specifically of the "second" or "redox-reactive" nucleotide moiety, as we will see in this paper.

Although the helix dipole has been discussed in various places (Blagdon & Goodman, 1975; Wada, 1976; Hol et al., 1978; Sheridan & Allen, 1980), it may be worthwhile to briefly summarize here some of its properties. The helix dipole originates from the individual dipole moments of the backbone peptide units. In the regular arrangement of an α-helix, the peptide dipole moments are all virtually parallel to the helix axis (Wada, 1976). The helix obtains, consequently, a large dipole moment. Hol et al. (1978) have shown that the electrostatic effect of the helix can be well approximated by placing a half positive unit charge near the N-terminus of a helix and a half negative unit charge near the C-terminus. The helix dipole can consequently interact favorably with charged moieties, and it appears that more than 20 helixes of proteins with known three-dimensional structures are involved in binding negatively charged phosphate moieties (Hol, 1985). Here we focus on an important subset of these helixes: those that bind dinucleotides.

In all enzymes referred to in the opening paragraph, the pyrophosphate group of the dinucleotide is located near the N-terminus of an α-helix. The structure of phosphorylase *b*, complexed with two molecules of NAD, as has recently been described by Stura et al. (1983), gives the first example of a different binding mode in this respect. The binding of NAD to site I is, as usually, stabilized by a favorable helix dipole–pyrophosphate interaction; however for the NAD binding to site N, this interaction is not involved. Apparently, the favorable helix dipole–pyrophosphate interaction has been replaced by other stabilizing forces.

In this paper we will only examine the structures of the dinucleotide–protein complexes whenever helixes play an important role, except for the NAD–phosphorylase *b* complex at site I. The main emphasis will be on the detailed interactions, such as hydrogen bonds, between the pyrophosphate and the helix N-terminus. Altogether, seven of such structural "close-ups", comprising six different enzymes and three different coenzymes, were available (Table I). In this study we have addressed the following questions: (a) How many hydrogen bonds occur between the pyrophosphate moiety and the main-chain atoms of the helix N-terminus? (b) Is there a specific orientation of the dinucleotide with respect to its binding helix? (c) Do the dinucleotide binding helixes belong to a particular folding unit? (d) Does the pyrophosphate binding helix, or folding unit, have a characteristic amino acid sequence?

Materials and Methods

For the analysis of the position of the pyrophosphate moiety with respect to the N-terminus of the α-helix, we used coordinates of six different enzymes: ADH,[1] LDH, GPD, PHBH, GRS, and DHFR. The source of these enzymes and the origin of the atomic coordinates are summarized in Table I. The accuracy of the coordinates varies considerably. The DHFR structure is known with greatest detail since it has been obtained by refinement with high-resolution data. The GPD coordinates probably have the lowest accuracy since they are obtained from a 3-Å electron density map.

The coordinates of the complexes of *Bacillus stearothermophilus* GPD (NAD) (Biesecker et al., 1977), chicken liver DHFR (NADP) (Volz et al., 1982), and porcine sMDH (NAD) (Webb et al., 1973) were not available to us. It has been reported that these structures are very similar to respectively the complexes of lobster GPD (NAD), *Lactobacillus casei* DHFR (NADP), and dogfish LDH (NAD).

Since in GRS the binding site of FAD as well as of NADP is known, we were able to analyze seven different dinucleotide binding sites. In DHFR, two helixes point toward the pyrophosphate moiety; therefore, the atomic arrangement at the N-terminus of eight helixes could be studied.

[1] Abbreviations: ADH, alcohol dehydrogenase; LDH, lactate dehydrogenase; GPD, glyceraldehyde-3-phosphate dehydrogenase; PHBH, *p*-hydroxybenzoate hydroxylase; GRS, glutathione reductase; DHFR, dihydrofolate reductase; rms, root mean square.

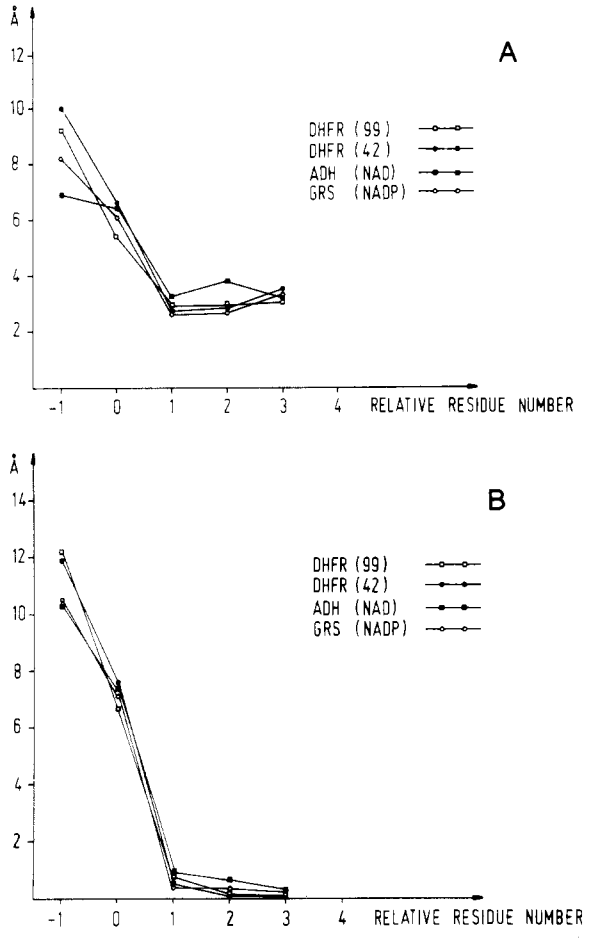

FIGURE 1: Determination of the first residue of dinucleotide binding helixes. (a) Distances (Å) between peptide carbonyl oxygens, O_i, and peptide nitrogens, N_{i+4}. Plotted are the distances for the oxygen atoms of two residues before and two residues beyond the beginning of four phosphate binding helixes: DHFR (helix 99–106), DHFR (helix 42–48), ADH (helix 201–212), and GRS (NADP, helix 196–208). The horizontal axis gives "relative" residue numbers; i.e., the residue corresponding to the first residue of the ideal helix obtains number 1. (b) Results of the superposition of the ideal helix ($\varphi = -64°$, $\psi = -41°$) onto four dinucleotide binding helixes. The vertical axis gives the distances (Å) between the corresponding C_α atoms of the ideal helix and the dinucleotide binding helix. It is obvious that the initial residue of the helix in the proteins can be defined unambiguously by means of these two plots. This appeared to be equally well possible for the other four helixes investigated in this article.

For the comparison, these eight helixes were superimposed onto an ideal α-helix, with $\varphi = -64°$ and $\psi = -41°$. The first residue of each helix was defined as the first residue of which the carbonyl oxygen atom participates in the hydrogen-bonding pattern of the α-helix. With this criterion the beginning of the helix could in all cases be established without doubt, as is illustrated in Figure 1A. The main-chain atoms N, C_α, and C, as well as the carbonyl oxygen atom, were used for the calculation of the best superposition of each α-helix onto the ideal α-helix. The refinement of this superposition, according to Rao & Rossmann (1973), was carried out in a number of cycles. At the end of each cycle, those atoms that deviated by more than 3 times the standard deviation were removed from the calculations. Table II identifies which residues were used for the superposition calculations; also, the root mean square positional differences of those atoms used in the final cycle are given.

The assignment of the first helix residue was further checked by an analysis as illustrated in Figure 1B. This figure shows, after superposition, the distances between corresponding atoms of the ideal α-helix and the dinucleotide binding α-helix. The data in Figure 1B illustrate that the C_α atoms of the residues before the first helix residue deviate substantially from the ideal helix positions.

Table II: Helixes Used for Superposition on Ideal α-Helix

enzyme	dinucleotide	helix	rms deviation (Å)[a]
ADH	NAD	201–212	0.3
LDH	NAD	29–39	0.2
GPD	NAD	9–21	0.6
PHBH	FAD	11–21	0.5
GRS	FAD	29–40	0.4
GRS	NADP	196–208	0.4
DHFR	NADP	42–48	0.2
DHFR	NADP	99–106	0.1

[a] Deviation of C_α atoms from ideal helix.

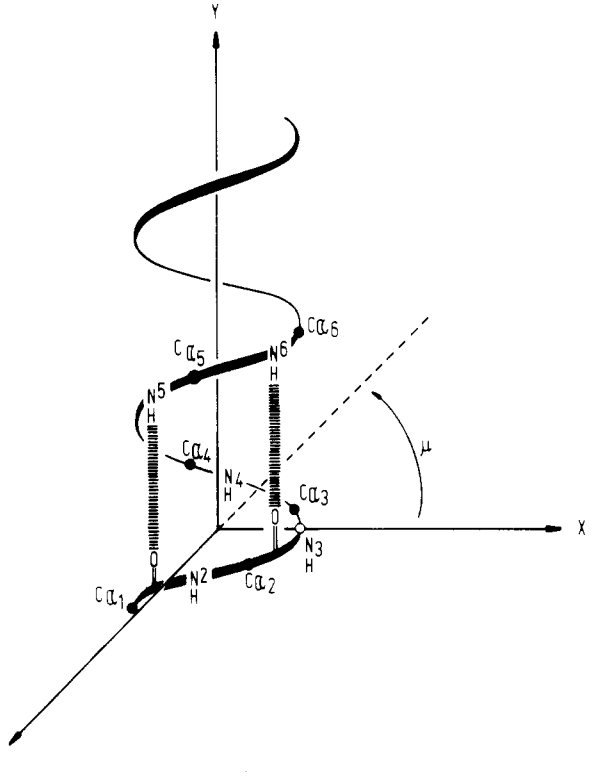

FIGURE 2: Definition of the coordinate system of the ideal α-helix. The helix axis coincides with the y axis; the C-terminus points toward the positive y axis. N_3, the nitrogen atom of the second peptide unit, lies on the positive x axis. μ defines the angle between the positive x axis and another vector in the XZ plane. A positive value for μ correlates with a right-handed screw around the y axis; e.g., μ (C_{α_3}) $\approx 30°$ and μ (C_{α_4}) $\approx 130°$.

In order to simplify the comparisons, the ideal helix had been positioned at the origin of an orthogonal coordinate system, such that the helix axis is parallel with the y axis, as is defined further in Figure 2. The peptide protons of the second, third, and fourth residue of the α-helix do not participate in the hydrogen bonds of the α-helix and are therefore, in principle, available for hydrogen bonds with substrate molecules.

Results

The close interaction of the helix N-terminus with the pyrophosphate moiety is clearly visualized in the gallery of stereo pictures (Figure 3) showing the seven helix–dinucleotide complexes that will be discussed in more detail in the next paragraphs. We like to follow the four questions posed in the introduction. For sake of convenience, they are repeated here before describing the results of our comparison.

(*a*) *How Many Hydrogen Bonds Occur between the Pyrophosphate Moiety and the Main-Chain Atoms of the Helix N-Terminus*? The number and lengths of hydrogen bonds

Table III: Possible Hydrogen Bonds, Shorter Than 3.4 Å, between the Pyrophosphate Oxygens and the Peptide Protons of the N-Terminus of the Helix[a]

enzyme	dinucleotide	helix	$O_{5'A}$	O_{1A}	O_{2A}	O_3	O_{1N}	O_{2N}	$O_{5'N}$
ADH	NAD	201–213					N203, 3.3; N202, 3.4		
LDH	NAD	29–39					N31, 3.4		
GPD	NAD	9–21					N11, 2.4		
PHBH	FAD	11–21						N13, 3.4	
GRS	FAD	29–40						N31, 2.7	
GRS	NADP	196–208						(N198, 3.6); (N199, 3.6)	
DHFR	NADP	42–48	N44, 3.4		N45, 3.2; N99, 3.0				
DHFR	NADP	99–106		N99, 3.1; (N100, 3.8); N101, 3.4; N102, 3.2				N101, 2.9; N100, 3.2	

[a] Distances larger than 3.4 Å (in parentheses) have been added for sake of completeness.

between the pyrophosphate moiety and the α-helix N-terminus for the six dinucleotide–enzyme complexes are given in Table III. The nomenclature of the pyrophosphate atoms is described in Figure 4. Except for DHFR, four common features become evident.

First, either the O_{1N} or the O_{2N} atom of the nicotinamide phosphate, P_N, is closest to the N-terminal NH groups of the dinucleotide binding helix. Second, usually only *one* hydrogen bond is formed. Third, this hydrogen bond is often rather long–over 3.2 Å in about half of the cases. Fourth, the hydrogen bond of O_{1N} or O_{2N} is consistently made with the hydrogen atom of N3 (as defined in Figure 2), which is the NH group of the second peptide unit of the dinucleotide binding helix.

These four features do not hold for the protein–pyrophosphate interactions in DHFR. In this case, O_{1A} can make altogether four relatively weak H-bonds with N1, N2, N3, and N4 of helix 99–106, while O_{2N} makes at least one good H-bond with N3 of this helix (see also Figure 3G).

It may be pointed out that the three NAD binding proteins all have O_{1N} interacting with the helix, whereas both FAD and NADP binding proteins interact with O_{2N}. It appears that in these cases there is no "ring" of N-terminal α-helical NH groups that interacts in a highly characteristic way with the pyrophosphate oxygen atoms. The number and strength of observed H-bonds between the pyrophosphate oxygens and the peptide NH groups of the α-helix N-terminus are clearly not optimal. This suggests that the general interaction of the negative charge of the pyrophosphate with the α-helix dipole field is the driving force for the conserved position of the pyrophosphate moiety near the α-helix N-terminus. The negative charge on the pyrophosphate is in all these cases partly compensated by the helix dipole field. As is shown in Table IV only in ADH, LDH, PHBH, and DHFR, this negative charge is further neutralized by the presence of positive side chains. In GPD and GRS (NADP), no charged side chains come close to the pyrophosphate moiety while in GRS (FAD) Asp-331 is the only charged side chain nearby. Clearly, the presence of positively charged side chains is not a conserved feature in the mode of binding of dinucleotides to these proteins.

(*b*) *Is There a Specific Orientation of the Dinucleotide with Respect to Its Binding Helix*? In order to compare the orientation of the various dinucleotides with respect to their α-helix, this helix was superimposed onto an ideal helix whose axis was chosen to be coincident with the *y* axis of a Cartesian coordinate system (see Materials and Methods). The helixes used for superposition have been defined in Table II. In Figure 5, six dinucleotides are shown simultaneously—rotated and translated according to the superposition of their binding helix onto the ideal helix–together with the actual helix of PHBH.

Table IV: Charged Side Chains within 4 Å of Pyrophosphate Oxygen Atoms

enzyme	dinucleotide	total charge due to side chains	residue
ADH	NAD	2+	Arg-369, Arg-47
LDH	NAD	1+	Arg-99
GPD	NAD	0	
PHBH	FAD	1+	Arg-42, Arg-44, Asp-286
GRS	FAD	1–[a]	Asp-331
GRS	NADP	0	
DHFR	NADP	1+	Arg-44

[a] Schulz et al. (1982) have discussed the possible presence of metal ions near the pyrophosphate moiety.

The constant position of the ADP moiety is striking. In contrast, considerable variation exists in the positions of the nicotinamide and isoalloxazine rings. Furthermore, in DHFR, omitted from these two figures, the dinucleotide has quite different orientations with respect to the binding helixes as is shown in Figure 6.

A projection of four selected dinucleotide atoms on a plane perpendicular to the helix axis for all eight dinucleotide binding helixes is given in Figure 6. It appears that all adenine moieties come close together in a region with $\mu \approx 150°$ (Figures 2 and 6). The two dihydrofolate reductase helixes do not evidently follow this pattern. Differences between the NADPH–DHFR and NADH–LDH interaction have also been discussed by Matthews et al. (1979). We will refer to the helixes of ADH, LDH, GPD, PHBH, and GRS as "category I helixes". As to the nicotinamide and isoalloxazine positions bound by these five enzymes, it appears that two values of μ are preferred: $\mu \approx 50°$ and $\mu \approx 0°$. The first group of μ values is found for the NAD binding proteins *and* corresponds with the O_{1N} atom being closest to the helix. The second group of μ values corresponds with NADP and FAD binding proteins *and* with the O_{2N} atom being closest to the α-helix.

For the category I helixes, it is therefore possible to speak of two distinct classes of dinucleotide binding modes: "class a" ($\mu \approx 50°$) and "class b" ($\mu = 0°$). Class a can be easily converted into class b by a simple left handed rotation of about 120° around the O_3–P_N bond. This is shown in Figure 7. It is evident that further studies on dinucleotide binding proteins are required to verify this distinction into two classes—and the simple relationship between them. Fortunately, several structural studies on enzyme–dinucleotide complexes are under way (Adams et al., 1983; Sheriff et al., 1982; Schierbeek et al., 1983).

(*c*) *Do the Dinucleotide Binding Helixes Belong to a Particular Folding Unit*? The six category I pyrophosphate binding helixes in ADH, LDH, GPD, PHBH, and GRS all belong to a highly similar βαβ fold. The DHFR helixes are

Table V: Pairwise Structural Comparison of Category I ADP Binding $\beta\alpha\beta$ Folds[a]

	ADH	LDH	GPD	PHBH	GRS (FAD)	GRS (NADP)
ADH		1.1	1.2	1.2	1.0	1.1
LDH	1.6		1.2	1.4	1.4	1.3
GPD	2.2	2.5		1.4	1.5	1.5
PHBH	1.4	1.9	2.2		0.9	0.8
GRS (FAD)	1.4	2.4	2.5	1.2		0.9
GRS (NADP)	1.9	2.1	2.3	1.2	2.0	

[a] The best superposition was calculated with all 27 common C_α atoms, as defined in the legend of Table VII. (Upper right) rms difference (Å) of the 27 common C_α atoms; (lower left) rms difference (Å) of the ADP moieties, after best superposition of the C_α atoms.

Table VI: Pairwise Sequence Comparison of the Category I ADP Binding $\beta\alpha\beta$ Folds[a]

	ADH	LDH	GPD	PHBH	GRS (FAD)	GRS (NADP)
ADH		7	5	6	7	3
LDH	1.1		9	3	8	5
GPD	1.1	1.0		5	7	4
PHBH	1.3	1.2	1.2		6	5
GRS (FAD)	1.1	1.0	1.3	1.1		4
GRS (NADP)	1.3	1.1	1.3	1.2	1.0	

[a] (Upper right) Number of identical residues of the 27 common residues, as defined in the legend of Table VII; (lower left) minimum base change per codon for the 27 common residues.

a distinct exception. Figure 8B shows the "deviating" main-chain fold near the phosphate binding (42–48) helix in DHFR. Figure 8A is a stereopicture of the $\beta\alpha\beta$ fold in PHBH as an example of the six common $\beta\alpha\beta$ units. In this latter example, it has been shown in sections a and b, above, that it is an oxygen atom of the "second" phosphate, P_N, that is most tightly associated with the α-helix. This $\beta\alpha\beta$ fold will therefore be referred to as an "ADP binding $\beta\alpha\beta$ fold".

The first DHFR phosphate binding helix (42–48) does form a $\beta\alpha\beta$ fold, but this fold is not so compact as the ADP binding $\beta\alpha\beta$ fold of PHBH (Figure 8). This is clearly the consequence of changes at crucial positions in the amino acid sequence, which will be discussed in the next section. The second DHFR phosphate binding helix is not part of a $\beta\alpha\beta$ unit.

The structural similarities of the six compact $\beta\alpha\beta$ folds are summarized in Table V. For this comparison, the $\beta\alpha\beta$ folds were pairwise superimposed on each other, using the 27 common C_α atoms, as defined in the legend of Table VII. It is quite remarkable that sequences that are so dissimilar (Table VI) do form such similar folds: the average rms differences is 1.2 Å. The largest rms differences, of 1.5 Å, is found between GPD and GRS (FAD) and between GPD and GRS (NADP). These two $\beta\alpha\beta$ pairs have respectively seven and four identical residues out of 27. For PHBH and LDH with only three identical residues out of 27 corresponding positions, a rms difference of 1.4 Å is found. Not only do the six $\beta\alpha\beta$ folds superimpose remarkably well, this is also true for the ADP moieties of the bound dinucleotides (Table V). With the 27 common protein C_α atoms for the optimal alignment, the rms difference for the ADP atoms varies between 1.2 and 2.5 Å, with an average rms difference of 1.9 Å.

(d) Does the Pyrophosphate Binding Helix, or Folding Unit, Have a Characteristic Amino Acid Sequence? The only common feature of all eight pyrophosphate binding helixes is a glycine at the N-terminus (Table VII). However, the amino acid sequences of the ADP binding $\beta\alpha\beta$ folds of ADH, LDH, GPD, GRS, and PHBH (Table VII) do have more common features. Since this $\beta\alpha\beta$ fold provides almost all the contacts for ADP binding, its sequence, in fact, does fulfill two re-

Table VII: Sequence Comparison of ADP Binding $\beta\alpha\beta$ Folds of Category I Dinucleotide Binding Proteins[a]

		ref
	β β β β β β α α α α α α α α α α α α β β β β β β	
	194 204 214 223	
ADH (NAD)	T C A V F G L G G V G L S V I M G C K A A G A A - R I I G V D I	Jörnvall, 1970
	Δ □ □ ● ● ● □ □ □ □ θ	
	22 32 42 52	
LDH (NAD	K I T V V G V G A V G M A C A I S I L M K D L A D E V A L V D V	Taylor, 1977
	Δ □ □ ● ● ● □ □ □ □ θ	
	2 12 22 31	
GPD (NAD)	K I G I D G F G R I G R L V L R A A L S C G A Q - V V A V N D P	Davidson et al., 1967
	Δ □ □ ● ● ● □ □ □ □ θ	
	4 14 24 32	
PHBH (FAD)	Q V A I I G A G P S G L L L G Q L L H K A G I - - D N V I L E R	Weijer et al., 1982
	Δ □ □ ● ● ● □ □ □ □ θ	
	22 32 42 50	
GRS (FAD)	D Y L V I G G G S G G L A S A R R A A E L G A - - R A A V V E S	Krauth-Sieghel et al., 1982
	Δ □ □ ● ● ● □ □ □ □ θ	
	189 199 209 217	
GRS (NADP)	R S V I V G A G Y I A V E M A G I L S A L G S - - K T S L M I R	Krauth-Sieghel et al., 1982
	Δ □ □ ● ● ● □ □ □ □ θ	
	β β β β β β α α α α α α α α α α α α β β β β β β	

[a] The fingerprint positions, as discussed in the text, are indicated below every given sequence. Residues at fingerprint positions with deviating properties are underlined. The 27 common residue positions used in the comparisons of the ADP binding $\beta\alpha\beta$ folds refer to, for example, 194–214 and 218–223 in ADH.

Table VIII: Compilation of All Known Sequences of Enzymes Homologous to ADH, LDH, or GPD[a]

		no. of identical residues (out of 27)	ref
	173 183 193 201		
ADH (yeast) (NAD)	V A I S G A A G G L G S L A V Q Y A K A M G Y - - R V L G I D G	9	Jörnvall, 1977
	Δ □ □ ● ● ● □ □ □ □ ⊖		
	9 19 29 38		
ADH (drosophila) (NAD)	V I F V A G L G G I G L D T S K Q L L K R D L K - N L V I L D R	8	Thatcher et al., 1980; Kreitman, 1983
	Δ □ □ ● ● ● □ □ □ □ ⊖		
	9 19 29 38		
ADH (drosophila) (NAD, inactive)	V I F V A D L G G I G L D T S K Q L L K R D L K - N L V I L D R	7	Thatcher, 1980
	Δ □ □ ● ● ● □ □ □ □ ⊖		
	9 19 29 38		
ADH (rat liver) (NAD)	T C A V F G L G G V G L S V V I G C K T A G A A - K I I A V D I	21	Eklund et al., 1976
	Δ □ □ ● ● ● □ □ □ □ ⊖		
	8 18 28 38		
LDH (*B. stearothermophilus*) (NAD)	R V V V I G A G F V G A S Y V F A L M N Q G I A D E I V L I D A	8	Schär et al., 1979
	Δ □ □ ● ● ● □ □ □ □ ⊖		
	8 18 28 38		
LDH (*B. caldotenax*) (NAD)	R V A V V G R G F V G A S Y A F A L M N Q G I A D E I V L I D A	10	Schär et al., 1979
	Δ □ □ ● ● ● □ □ □ □ ⊖		
	7 17 27 37		
LDH (*Bacillus* X_1) (NAD)	K V A L I G A G F V G S S Y V F A L I N Q G I T D E L V V I D L	7	Schär et al., 1979
	Δ □ □ ● ● ● □ □ □ □ ⊖		
	20 30 40 50		
LDH (mouse testes) (NAD)	K I T V V G V G D V G M A C A I S I L L K G L A D E L A L V D A	24	Pan et al., 1983
	Δ □ □ ● ● ● □ □ □ □ ⊖		
	21 31 41 51		
LDH (M, pig) (NAD)	K I T V V G V G A V G M A C A I S I L M K E L A D E I A L V D V	26	Kilz et al., 1977
	Δ □ □ ● ● ● □ □ □ □ ⊖		
	22 32 42 52		
LDH (H, pig) (NAD)	K I T V V G V G Q V G M A C A I S I L G K S L T D E L A L V D V	23	Kilz et al., 1977
	Δ □ □ ● ● ● □ □ □ □ ⊖		
	3 13 23 33		
GPD (*B. stearothermophilus*) (NAD)	K V G I N G F G R I G R N V F R A A L K N P D I E V V A V N D L	20	Biesecker et al., 1977
	Δ □ □ ● ● ● □ □ □ □ ⊖		
	2 12 22 32		
GPD (*T. aquaticus*) (NAD)	K V G I N G F G R I G R Q V F R I I H S R G V E - V A L I N D L	16	Hocking et al., 1976
	Δ □ □ ● ● ● □ □ □ □ ⊖		
	2 12 22 32		
GPD (yeast) (NAD)	R V A I N G F G R I G R L V M R I A L S R P V V E V V A L N D P	19	Holland et al., 1980
	Δ □ □ ● ● ● □ □ □ □ ⊖		
	2 12 22 32		
GPD (pig) (NAD)	K V G V D G F G R I G R L V T R A A F N S G K V D I V A I N D P	20	Harris et al., 1968
	Δ □ □ ● ● ● □ □ □ □ ⊖		

[a] Residues at fingerprint positions with deviating properties are underlined. The third column contains the number of identical residues with respect to the 27 common amino acids of the βαβ fold (see legend to Table VII) in the homologous enzyme with known structure.

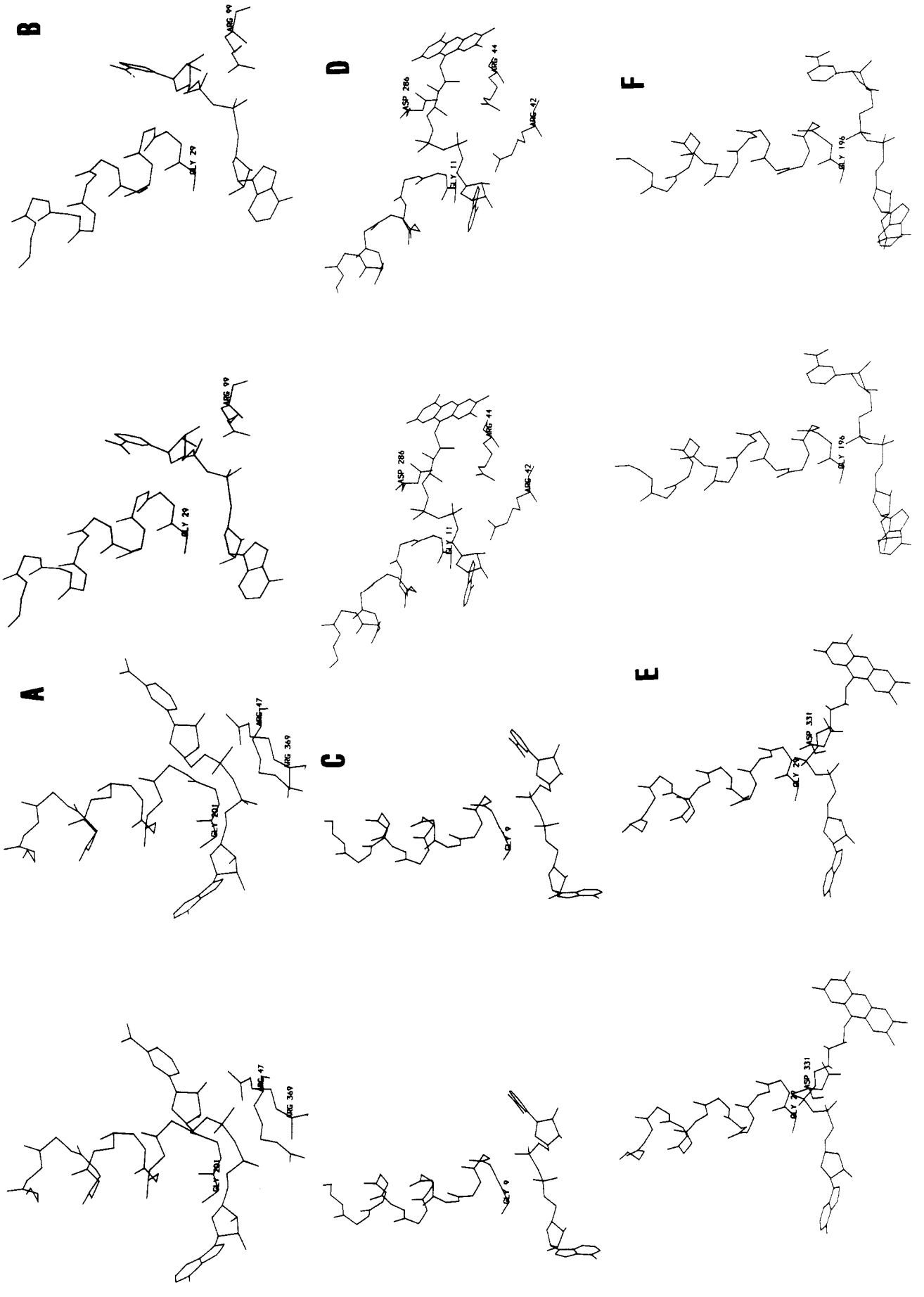
B
ARG 99
GLY 29
D
ASP 286
ARG 44
GLY 11
ARG 42
F
GLY 196
ARG 99
GLY 29
ASP 286
ARG 44
GLY 11
ARG 42
GLY 196
A
ARG 47
ARG 369
GLY 201
C
GLY 9
E
ASP 331
GLY 29
ARG 47
ARG 369
GLY 201
GLY 9
ASP 331
GLY 29

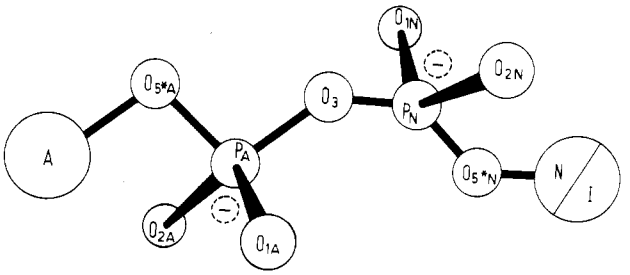

FIGURE 4: Nomenclature of the pyrophosphate moiety: A, adenine; N, nicotinamide; I, isoalloxazine.

quirements: it results in (1) a similar fold with (2) similar binding properties. These two requirements impose a certain constraint on the sequence, which made it possible to deduce a "fingerprint" that describes its characteristics (Wierenga & Hol, 1983). This fingerprint of the ADP binding $\beta\alpha\beta$ fold is as follows:

(i) Three conserved glycine residues have the sequence Gly-X-Gly-X-X-Gly in the region connecting the first β-strand with the α-helix. The first of these glycines is, so far, entirely conserved in all known structures. It allows for a tight turn of the main chain, with special (φ, ψ) angles as is shown in Figure 9. The second of the three glycines is conserved because steric hindrance with the bound dinucleotide would occur with a side chain at this position. A glycine at this position also allows for φ and ψ values outside the range acceptable for residues with large side chains (Figure 9). In only one case, sMDH (Birktoft et al., 1982), an alanine instead of a glycine does occur. However, this alanine is part of an "X-ray sequence". So far, no chemically determined sequence has been published. The third conserved glycine residue is important to provide space for a close interaction between the β-strands and the α-helix. Only in sMDH and in the NADP binding $\beta\alpha\beta$ fold of GRS does an alanine occur instead of a glycine. In the latter case, this explains the relatively large deviation of the main chain of GRS at this position (1.9 Å) after superposition of the GRS nucleotide binding fold onto the PHBH nucleotide binding fold (see Table VIII; Wierenga et al., 1983). In DHFR, the first and third glycines are replaced by a valine and threonine at helix 42–49 and by an alanine and isoleucine at helix 99–107 (Table VII). Therefore, these helixes cannot be part of a compact $\beta\alpha\beta$ fold.

(ii) Six predominantly hydrophobic residues at positions indicated by squares in Table VII form the hydrophobic core of the $\beta\alpha\beta$ unit. They are usually rather small.

(iii) A conserved negatively charged residue is present at the C-terminus of the second β-strand for the $\beta\alpha\beta$ units binding NAD or FAD. This Asp or Glu residue forms hydrogen bonds with the 2′-hydroxyl group of the adenine ribose moiety. For NADP binding $\beta\alpha\beta$ units, this interaction is absent because of the presence of the 2′-phosphate moiety. In DHFR, Arg-43 interacts, instead, with the 2′-phosphate of NADP. In GRS, His-219 interacts with the 2′-phosphate group of NADP.

(iv) A conserved hydrophilic residue is present at the N-terminus of the first β-strand (In Table VII). The function of this residue is not obvious.

The fingerprint, discussed above, allows the localization of the dinucleotide binding $\beta\alpha\beta$ folds in other proteins of known sequence. As a further confirmation of the fingerprint, Table VIII contains the presumed dinucleotide binding $\beta\alpha\beta$ units of all known homologous sequences of ADH, LDH, and GPD, together with the fingerprint identifiers. Despite the large variation in sequence homology, only the mutated *Drosophila* ADH sequence truly violates the rules of the fingerprint. In this sequence, the first unique glycine has been replaced by

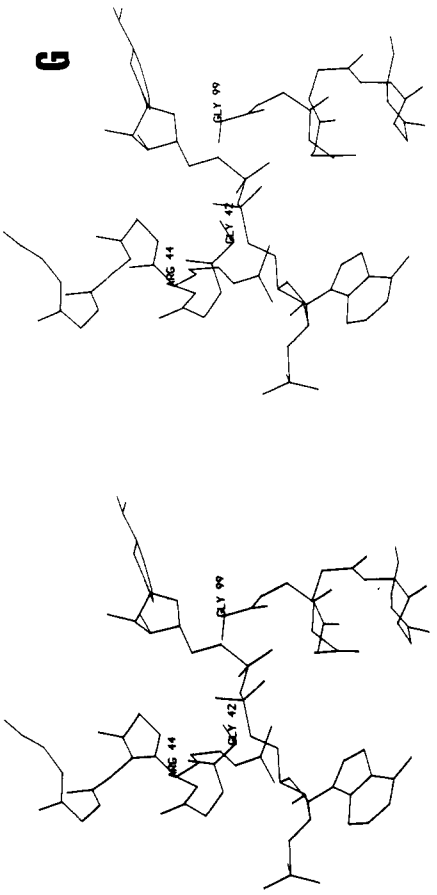

FIGURE 3: Gallery of eight phosphate binding helixes. Included are also the positions of the charged residues, which have atoms within 4 Å of the pyrophosphate moiety (see Table IV). (A) ADH (NAD, helix 201–212); (B) LDH (NAD, helix 29–39); (C) GPD (NAD, helix 9–21); (D) PHBH (FAD, helix 11–21); (E) GRS (FAD, helix 29–40); (F) GRS (NADP, helix 196–208); (G) DHFR (NADP, helix 42–48 and helix 99–106). These figures, as well as Figures 5, 7, and 8, were made by using an interactive computer graphics system (Brandenburg et al., 1981).

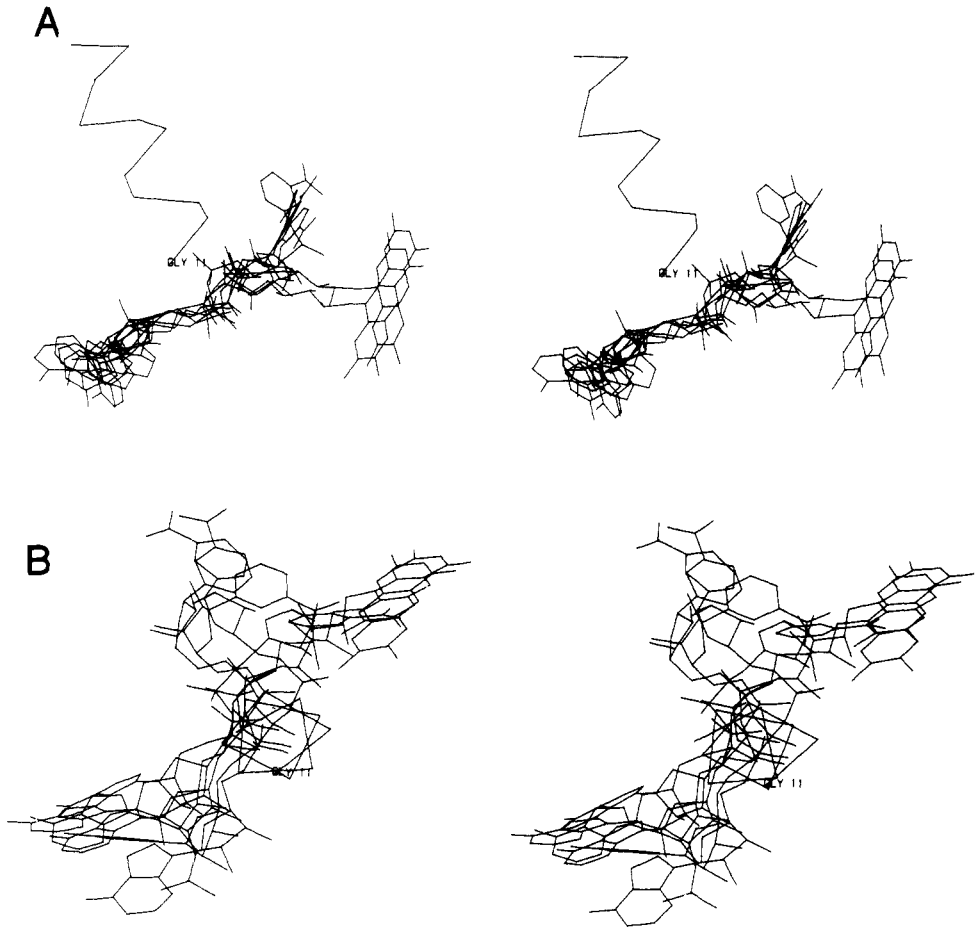

FIGURE 5: Relative positions of the dinucleotides bound by the category I helixes: ADH (NAD), LDH (NAD), GPD (NAD), PHBH (FAD), GRS (FAD), and GRS (NADP) after superposition of their phosphate binding helixes onto the ideal α-helix. Only the PHBH helix is shown. (A) The helix axis parallel to the plane of the paper; (B) the helix viewed end on, with the N-terminus furthest away.

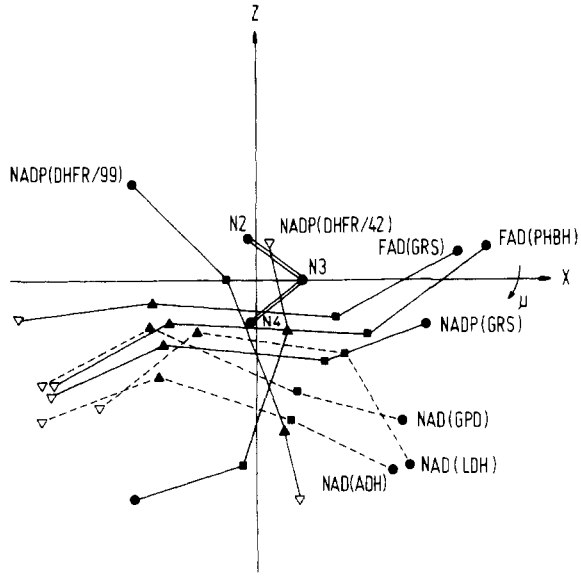

FIGURE 6: Relative position, projected on the *XZ* plane defined in Figure 2, of selected dinucleotide atoms after superposition of their phosphate binding helixes on the ideal α-helix. N2, N3, and N4 are the projected positions of the peptide nitrogen atoms of the ideal α-helix. (●) N_1 (nicotinamide) or N_{10} (isoalloxazine); (■) C_5* (nicotinamide ribose or isoalloxazine ribitol); (▲) C_5* (adenine ribose); (▽) N_9 (adenine). $\bar{\mu}$ [N_1, N_{10} of NADP (GRS), FAD] = 0°; $\bar{\mu}$ (N_1 of NAD) = 50°; $\bar{\mu}$ [N_9 of NAD, FAD, NADP (GRS)] = 150°. Except for DHFR, the adenine moieties superimpose well. The NAD nicotinamide moieties form class a (dashed lines); the isoalloxazine rings and the NADP nicotinamide moiety from class b (solid lines, excluding DHFR).

an aspartic acid. This replacement undoubtedly does not allow for the tight $\beta\alpha\beta$ fold, which explains why this ADH is inactive. Also, the yeast ADH sequence deviates somewhat near residues 173–183. In the published alignment with horse liver ADH (Jörnvall, 1977), Ala-179 is considered as an insertion. All 12 other sequences closely follow the fingerprint in agreement with the folds predicted for these sequences in the original litterature (see Table VIII).

Discussion

Previously, it has been pointed out (Hol et al., 1978) that the favorable interaction of the helix dipole with the pyrophosphate moiety of a dinucleotide is an important stabilizing factor for the formation of these complexes. So far, these interactions in the various known structures have been compared only in a rather qualitative way. Therefore, we have analyzed and determined the essential structural features of these complexes in a much more detailed and quantitative manner.

The eight helixes analyzed in this paper fall clearly into different groups. Category I consists of those dinucleotide binding helixes that are part of a compact $\beta\alpha\beta$ unit (Figure 8A). The two remaining helixes are found in DHFR; one helix is part of a "distorted" or "loose" $\beta\alpha\beta$ unit (Figure 8B), while the second one is not incorporated in a protein segment with a supersecondary structure. It is obviously premature to assign these two helixes to other categories.

It apears that in category I the ADP moiety of the dinucleotide is bound to the compact $\beta\alpha\beta$ unit in a highly conserved manner. More variability exists as to the binding

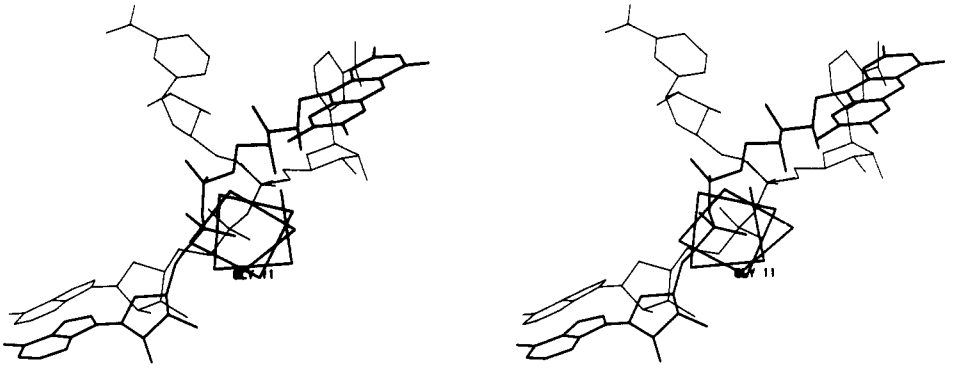

FIGURE 7: Two orientations of NAD (LDH): before and after a left-handed rotation of 120° around the O_3–P_N bond. FAD (PHBH) and the phosphate binding helix of PHBH are shown in thick lines. The N-terminus points furthest away. Previous to the O_3–P_N rotation, the nicotinamide as bound by LDH does not coincide with the flavin ring of FAD.

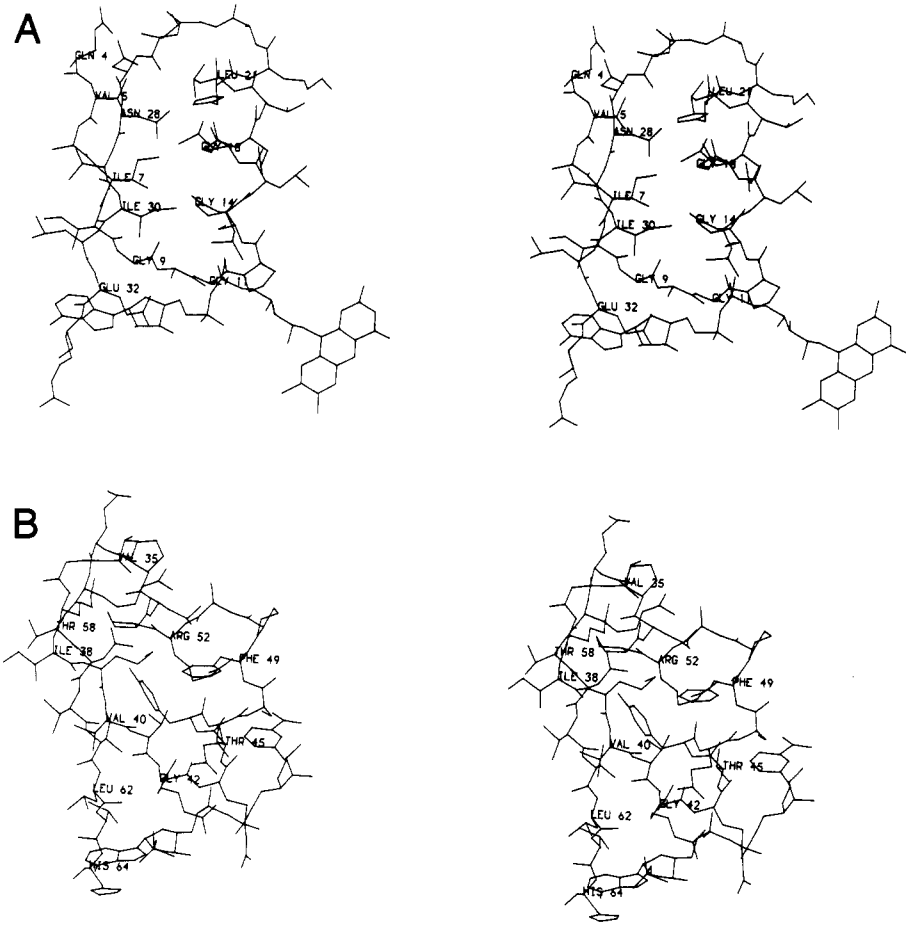

FIGURE 8: Dinucleotide binding $\beta\alpha\beta$ fold. (A) The compact ADP binding $\beta\alpha\beta$ fold of PHBH (4–33). This is an example of the six structurally related $\beta\alpha\beta$ folds of the category I dinucleotide binding proteins. Amino acids at fingerprint positions (Table VII) are labeled. (B) The loose $\beta\alpha\beta$ fold of DHFR (35–64).

mode of the "redox-reactive" nucleotide moiety of the dinucleotides. Here, two classes, class a and class b, have been defined.

Class a can be converted into class b by a left-handed rotation around the O_3–P_N bond. Because of this rotation, the redox-reactive moieties are at completely different positions with respect to the $\beta\alpha\beta$ fold. The nicotinamide moiety of class a is folded back toward the pleated sheet, while in class b the redox-reactive moiety is pointing away from this parallel sheet.

In previous comparative studies, notably by Rossmann et al. (1974) and Ohlsson et al. (1974), the conserved features of what we have called the class a enzymes have been discussed, while Schulz (1980) and Wierenga et al. (1983) have analyzed the class b structures. Most recently, Birktoft & Banaszak (1985) have discussed the dinucleotide binding folds extensively. They show that in fact a "β_D-strand" is present in all category I enzymes. This strand is hydrogen bonded to the first strand of the $\beta\alpha\beta$ fold and always has a glycine near its C-terminus.

Combining all these observations together one might conclude that the common structural elements of the category I helix containing dinucleotide binding folds form in fact an *ADP binding unit* with the $\beta\alpha\beta$ building block as its most prominent part. It is the pyrophosphate group of the ADP moiety that superimposes best (Figure 5). Subsequently, it is somewhat surprising to note in Table III that the conserved position of the P_N oxygen atom with respect to the peptide protons of the N-terminus of the category I helix does not allow for optimal

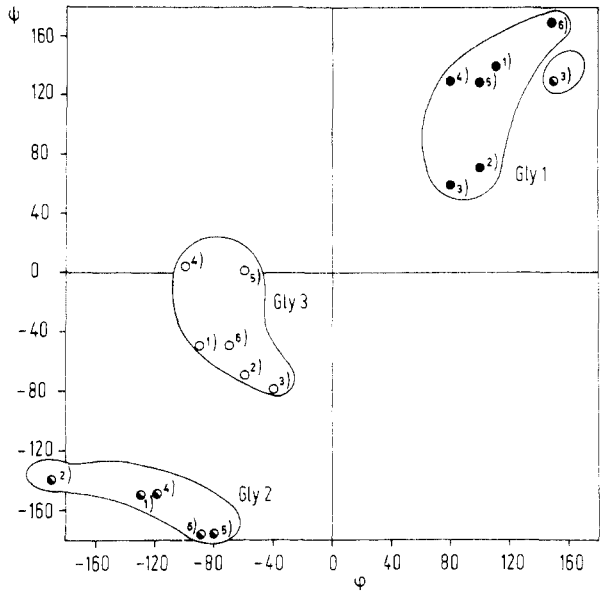

FIGURE 9: φ and ψ values of the three unique glycines in the fingerprint of the sequence Gly-X-Gly-X-X-Gly, indicated respectively by Gly 1 (●), Gly 2 (◐), and Gly 3 (○). The six ADP binding $\beta\alpha\beta$ folds are indicated by (1) GRS (FAD), (2) LDH (NAD), (3) GPD (NAD), (4) ADH (NAD), (5) PHBH (FAD), and (6) GRS (NADP). The abnormal Gly 2 position of GPD (NAD) might be due to inaccuracies of the coordinates.

hydrogen bonds, such as is, for example, the case to a much larger extent for the O_{1A} atom of NADP (DHFR) (Table III), which is surrounded by four peptide protons. Apparently, the general position of the pyrophosphate with respect to the helix is more important than an optimal hydrogen-bonding arrangement. This is clearly in accord with the importance of the favorable helix dipole–pyrophosphate interaction.

Although the helix N-termini discussed in this paper occur in active site clefts, they should be freely accessible for ligands. In this respect, it is interesting to observe that phosphate binding helixes almost always begin with a glycine. In DHFR, Gly-42 and Gly-99 are strictly conserved; their importance has been discussed by Matthews et al. (1979). Other examples are provided by, e.g., pyridoxal phosphate binding helixes: Gly-107 in aspartate amino transferase (J. N. Jansonius, personal communication) and Gly-134 in phosphorylase (Johnson et al., 1980). In fact, also many "active site helixes" (Hol et al., 1978; Hol, 1985) start with a glycine, e.g., Gly-298 in PHBH (Weijer et al., 1983), Gly-219 in subtilisin (Drenth et al., 1971), and Gly-23 in papain (Drenth et al., 1976). In all cases, the absence of a side chain at these positions probably allows for a close approach of the substrate to the helix N-terminus.

The accessibility of helix termini is obviously also influenced by the course of the loops of the main chain running into and out of the helix. For dinucleotide binding helixes, the main chain near the N-terminus does not obscure the helix axis (Figures 3, 6, and 8), but the loop at the C-terminus covers the helix axis. Dinucleotide binding helixes have apparently an "open" N-terminus.

Two major conclusions emerge from this study: (i) in all cases examined the general position of the pyrophosphate with respect to the helix N-terminus is highly conserved, while details of the interaction, such as H-bonds, show greater variability; (ii) the six category I helixes all belong to a compact $\beta\alpha\beta$ fold, with a characteristic amino acid sequence fingerprint, to which only the ADP moiety of the dinucleotide is bound in a highly conserved manner.

ACKNOWLEDGMENTS

We are indebted to Drs. G. E. Schultz, C. I. Brändén, and H. Eklund for making coordinates available to us. We also thank Prof. J. Drenth for stimulating discussions, R. A. Hogenkamp for typing the manuscript, and R. Kloosterman for the preparation of the line drawings.

Registry No. ADH, 9031-72-5; LDH, 9001-60-9; GPD, 9001-50-7; PHBH, 9059-23-8; GRS, 9001-48-3; DHFR, 9002-03-3; FAD, 146-14-5; NAD, 53-84-9; NADP, 53-59-8; ADP, 58-64-0.

REFERENCES

Adams, M. J., Archibald, I. G., Bugg, C. E., Carne, A., Gover, S., Helliwell, J. R., Pickersgill, R. W., & White, S. W. (1983) *EMBO J. 2*, 1009–1014.

Bernstein, F. C., Koetzle, T. F., Williams, G. J. B., Meyer, E. F., Brice, M D., Rodgers, J. R., Kennard, O., Shimanoucki, T., & Tasumi, M. (1977) *J. Mol. Biol. 112*, 535–542.

Biesecker, G., Harris, J. I., Thierry, J. C., Walker, J. E., & Wonacott, A. J. (1977) *Nature (London) 266*, 328–333.

Birktoft, J. J., & Banaszak, L. J. (1985) *Protein Pept. Rev.* (in press).

Birktoft, J. J., Fernley, R. T., Bradshaw, R. A., & Banaszak, L. J. (1982) *Proc. Natl. Acad. Sci. U.S.A. 79*, 6166–6170.

Bitar, K. G., Blankenship, D. T., Walsh, K. A., Dunlap, R. B., Reddy, A. V., & Freisheim, J. H. (1977) *FEBS Lett. 80*, 119–122.

Blagdon, D. E., & Goodman, M. (1975) *Biopolymers 14*, 241–245.

Bolin, J. T., Filman, D. J., Matthews, D. A., Hamlin, R. C., & Kraut, J. (1982) *J. Biol. Chem. 257*, 13650–13662.

Brändén, C.-I. (1980) *Q. Rev. Biophys. 13*, 317–338.

Brandenburg, N. P., Dempsey, S., Dijkstra, B. W., Lijk, L. J., & Hol, W. G. J. (1981) *J. Appl. Crystallogr. 14*, 274–279.

Davidson, B. E., Sajgö, M., Noller, H. F., & Harris, J. I. (1967) *Nature (London) 216*, 1181–1185.

Drenth, J., Hol, W. G. J., Jansonius, J. N., & Koekoek, R. (1971) *Cold Spring Harbor Symp. Quant. Biol. 36*, 107–116.

Drenth, J., Kalk, K. H., & Swen, H. M. (1976) *Biochemistry 15*, 3731–3738.

Eklund, H., Brändén, C.-I., & Jörnvall, H. (1976) *J. Mol. Biol. 102*, 61–73.

Eklund, H., Samama, J.-P., Wallén, L., Brändén, C.-I., Åkeson, Å., & Jones, T. A. (1981) *J. Mol. Biol. 146*, 561–587.

Harris, J. I., & Perham, R. N. (1968) *Nature (London) 219*, 1025–1028.

Hocking, J. D., & Harris, J. I. (1976) in *Enzymes and Proteins from Thermophilic Microorganisms* (Zuber, H., Ed.) pp 121–133.

Hol, W. G. J. (1985) *Prog. Biophys. Mol. Biol.* (in press).

Hol, W. G. J., Van Duijnen, P. Th., & Berendsen, H. J. C. (1978) *Nature (London) 273*, 443–446.

Holland, J. P., & Holland, M. J. (1980) *J. Biol. Chem. 255*, 2596–2604.

Johnson, L. N., Jenkins, J. A., Wilson, K. S., Stura, E. A., & Zanotti, G. (1980) *J. Mol. Biol. 140*, 565–580.

Jörnvall, H. (1970) *Eur. J. Biochem. 16*, 25–40.

Jörnvall, H. (1977) *Eur. J. Biochem. 72*, 443–452.

Kilz, H. H., Keil, W., Griesbach, M., Petry, K., & Meijer, H. (1977) *Hoppe-Seyler's Z. Physiol. Chem. 358*, 123–127.

Krauth-Sieghel, R. L., Blatterspiel, R., Saleh, M., Schilz, E., Schirmer, R. H., & Untucht-Grau, R. (1982) *Eur. J. Biochem. 121*, 259–267.

Kreitman, H. (1983) *Nature (London) 304*, 412–417.
Matthews, D. A., Alden, R. A., Freer, S. T., Xuong, N., & Kraut, J. (1979) *J. Biol. Chem. 254*, 4144–4151.
Moras, D., Olsen, K. W., Sabeson, M. N., Buehner, M., Ford, G. C., & Rossmann, M. G. (1975) *J. Biol. Chem. 250*, 9137–9162.
Ohlsson, I., Nordström, B., & Brändén, C.-I. (1974) *J. Mol. Biol. 89*, 339–354.
Pan, Y. E., Sharief, F. S., Okabe, M., Huang, S., & Li, S. S. (1983) *J. Biol. Chem. 258*, 7005–7016.
Rao, S. T., & Rossmann, M. G. (1973) *J. Mol. Biol. 76*, 241–256.
Rossmann, M. G., Moras, D., & Olsen, K. W. (1974) *Nature (London) 250*, 194–199.
Rossmann, M. G., Liljas, A., Brändén, C.-I., & Banaszak, L. J. (1975) *Enzymes, 3rd Ed. 11*, 61–102.
Schär, H.-P., & Zuber, H. (1979) *Hoppe-Seyler's Z. Physiol. Chem. 360*, 795–807.
Schierbeek, A. J., Van der Laan, J. M., Groendijk, H., & Wierenga, R. K. (1983) *J. Mol. Biol. 165*, 563–564.
Schulz, G. E. (1980) *J. Mol. Biol. 138*, 335–347.
Schulz, G. E., Schirmer, R. H., & Pai, E. F. (1982) *J. Mol. Biol. 160*, 287–308.
Sheridan, R. P., & Allen, L. C. (1980) *Biophys. Chem. 11*, 133–136.
Sheriff, S., & Herriott, J. R. (1981) *J. Mol. Biol. 145*, 441–451.
Stura, E. A., Zanotti, G., Babu, Y. S., Sansom, M. S. P., Stuart, D. I., Wilson, K. S., Johnson, L. N., & Van de Werve, D. (1983) *J. Mol. Biol. 170*, 529–565.
Taylor, S. S. (1977) *J. Biol. Chem. 252*, 1799–1806.
Thatcher, D. R. (1980) *Biochem. J. 187*, 875–883.
Thatcher, D. R., & Sawyer, L. (1980) *Biochem. J. 187*, 884–886.
Volz, K. W., Matthews, D. A., Alden, R. A., Freer, S. T., Hansch, C., Kaufman, B. T., & Kraut, J. (1982) *J. Biol. Chem. 257*, 2528–2536.
Wada, A. (1976) *Adv. Biophys. 9*, 1–63.
Webb, L. E., Hill, R. J., & Banaszak, L. J. (1973) *Biochemistry 12*, 5101–5109.
Weijer, W. J., Hofsteenge, J., Vereijken, J. M., Jekel, P. K., & Beintema, J. J. (1982) *Biochim. Biophys. Acta 704*, 385–388.
Weijer, W. J., Hofsteenge, J., Beintema, J. J., Wierenga, R. K., & Drenth, J. (1983) *Eur. J. Biochem. 133*, 109–118.
White, J., Hackert, M. L., Buehner, M., Adams, M. J., Ford, G. C., Lentz, P. J., Smiley, I. E., Steindel, S. J., & Rossmann, M. G. (1976) *J. Mol. Biol. 102*, 759–779.
Wierenga, R. K., & Hol, W. G. J. (1983) *Nature (London) 302*, 842–844.
Wierenga, R. K., De Jong, R. J., Kalk, K. H., Hol, W. G. J., & Drenth, J. (1979) *J. Mol. Biol. 131*, 55–73.
Wierenga, R. K., Drenth, J., & Schulz, G. E. (1983) *J. Mol. Biol. 167*, 725–739.

Rate-Limiting Step in the Actomyosin Adenosinetriphosphatase Cycle: Studies with Myosin Subfragment 1 Cross-Linked to Actin

Leonard A. Stein,[‡] Lois E. Greene, P. Boon Chock, and Evan Eisenberg*

Laboratory of Cell Biology, National Heart, Lung, and Blood Institute, National Institutes of Health, Bethesda, Maryland 20205
Received May 15, 1984

ABSTRACT: Although there is agreement that actomyosin can hydrolyze ATP without dissociation of the actin from myosin, there is still controversy about the nature of the rate-limiting step in the ATPase cycle. Two models, which differ in their rate-limiting step, can account for the kinetic data. In the four-state model, which has four states containing bound ATP or ADP·P_i, the rate-limiting step is ATP hydrolysis (A·M·ATP $\rightleftharpoons$ A·M·ADP·P_i). In the six-state model, which we previously proposed, the rate-limiting step is a conformational change which occurs before P_i release but after ATP hydrolysis. A difference between these models is that only the four-state model predicts that almost no acto·subfragment 1 (S-1)·ADP·P_i complex will be formed when ATP is mixed with acto·S-1. In the present study, we determined the amount of acto·S-1·ADP·P_i formed when ATP is mixed with S-1 cross-linked to actin [Mornet, D., Bertrand, R., Pantel, P., Audemard, E., & Kassab, R. (1981) *Nature (London) 292*, 301–306]. The amount of acto·S-1·ADP·P_i was determined both from intrinsic fluorescence enhancement and from direct measurement of P_i. We found that at μ = 0.013 M, the fluorescence magnitude in the presence of ATP of the cross-linked actin·S-1 preparation was about 50% of the value obtained with S-1, while at μ = 0.053 M the fluorescence magnitude was about 70% of that obtained with S-1. If the ATP hydrolysis step were rate-limiting, the fluorescence magnitude should be less than 10% of that with S-1 alone. Control studies showed that almost none of the fluorescence increase was due to ATP binding. Furthermore, direct measurement of P_i corroborated the fluorescence studies. These results suggest that at both low and high ionic strength, the ATP hydrolysis step is not the rate-limiting step. Instead, the data are consistent with the rate-limiting step occurring before P_i release and after the ATP hydrolysis step, as proposed in the six-state kinetic model.

It is now generally accepted that muscle contraction is driven by the cyclic interaction of the two muscle proteins, actin and myosin, in the presence of ATP. Studies using the soluble proteolytic fragment of myosin, subfragment 1 (S-1),[1] have

[‡] Present address: Department of Cardiology, State University of New York at Stony Brook, Stony Brook, NY 11794.

[1] Abbreviations: S-1, subfragment 1 of myosin; acto-S-1, complex of actin with S-1; EDC, 1-ethyl-3-[3-(dimethylamino)propyl]carbodiimide; MES, 2-(*N*-morpholino)ethanesulfonic acid.